International Journal of Research in Engineering and Science (IJRES)
ISSN (Online): 2320-9364, ISSN (Print): 2320-9356
www.ijres.org Volume 10 Issue 6 ǁ 2022 ǁ PP. 1369-1375

Power Optimization Scheme for Electrical Vehicle by Using Fuzzy Logic Control of Induction Motor

K.DHEEKSHITHA, K.CHANDRAKANTH, G.JUNAID YASEEN, K.NAVYA SREE

[*1]K.Dheekshitha Student of EEE Department, SRIT-ATP
[2]K.Chandrakanth Student of EEE Department, SRIT-ATP
[3]G.Junaid Yaseen Student of EEE Department, SRIT-ATP
[4]K.Navya Sree Student of EEE Department, SRIT-ATP

Abstract
Present days using fossil gas vehicles accelerated appreciably that ends in growing the attention of CO2 in atmosphere. In order to lessen those effects, the opportunity is Electric Vehicle's (EV's). EV's have extra blessings than regular vehicle, those are extra environmentally pleasant and do now no longer produces any type of worldwide gases. In general, synchronous vehicles and induction vehicles are utilized in EV's however in exercise Induction vehicles are extra popular. Energy performance is vital as electricity garage is confined in EV's. These vehicles have the subsequent dangers like, much less performance, consumes extra electricity than the real want to carry out its running while it's far working in much less than complete load situation in EV's applications. To conquer those issues in induction vehicles, distinctive strategies like PID controllers and FUZZY Logic Controllers (FLC). The PID controllers have extra wide variety of remarks loops that sends the mistake indicators lower back to the enter in order that the mistakes are rectified, this method is time consuming. So on this project, it proposed to apply FLC strategies to enhance the overall performance of induction motor. By the use of FLC the beginning modern-day amplitude may be managed and extra electricity is saved. The proposed version tested via way of means of the use of MATLAB/SIMULINK software.

Keywords: Electric vehicle.PID Controller, Fuzzy Logic Controller, Membership function, Induction Motor

---

Date of Submission: 06-06-2022 Date of acceptance: 21-06-2022

I. INTRODUCTION

The heavy intake of fossil fuels has persisted to rise, mainly with inside the previous couple of decades, ensuing in an boom in CO2 stages with inside the atmosphere. Concerns approximately weather alternate and growing sea stages because of international warming are intensifying, making international efforts to lessen carbon dioxide an pressing requirement. With transport bills accounting for around 20% of global carbon dioxide emissions, big improvements in the performance of gasoline cars are essential. Electric vehicles (EVs) have many advantages, including improved performance, environmental friendliness, quiet operation and less reliance on electricity. Electric machines, on the alternative hand, are a possible alternative Electric machine, on the alternative hand, are a essential thing of any pressure, which includes those who can be included into EVs and hybrid EVs. The basic forms of machines that can be used in electric vehicles are synchronous cars and induction cars (IM). The following propulsion must be protected inside the EV pressure motor:

(i) High torque density to provide sufficient driving force when starting, climbing and accelerating.
(ii) High efficiency to prolong the static power speed range.
(iii) Strong flux regulation capability to extend the static power speed range.

Because of its strength, cheap cost, and minimal maintenance requirements, the IM is the greatest choice for EVs, but its losses are much larger in the EV application , resulting in a decrease in machine efficiency. Low energy density, heavier weight, longer charging periods and longer battery life are the most significant impediments to such cars being accepted into the transportation system. Therefore, the most efficient use of energy is essential for the operation of electric vehicles. Proportional integral derivative (PID) control, which is used in many industrial drives, is widely considered to be one of the most prevalent units due to its efficacy and ease of implementation. PID controllers are also employed in industrial applications and are used in most existing control loops. Significant performance deterioration may occur when changing operation circumstances owing to component obsolescence or a change in the working environment. Due to the unpredictability and complexity of modeling, the correct analytical model of a controlled system, intelligent control approaches such as fuzzy logic control (FLC) can give superior performance.

Many strategy rules are available in the FLC system that make use of linguistic tags in a more straightforward manner. This method has been employed in a variety of different EV. To begin, there is an electric motor system, in which there is generally just one electrical machine, which is usually a three-phase AC.

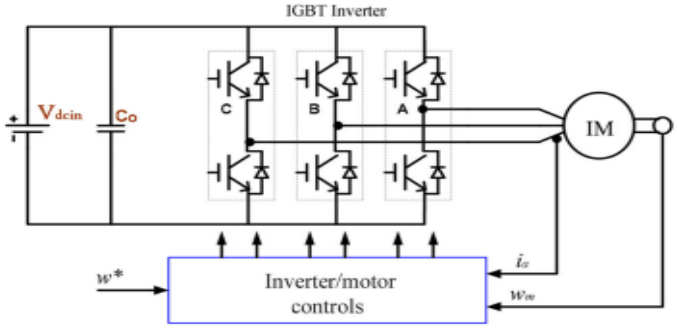

Fig. 1 EV drive with an IM

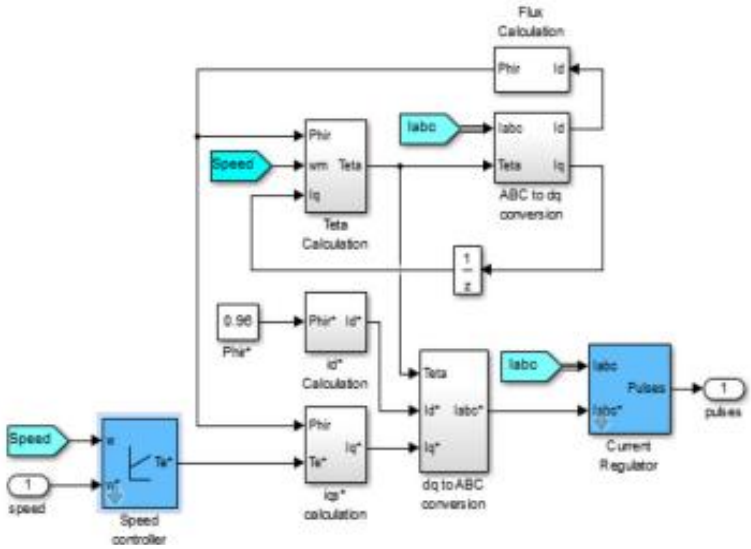

Fig. 2 Induction Motor Control system

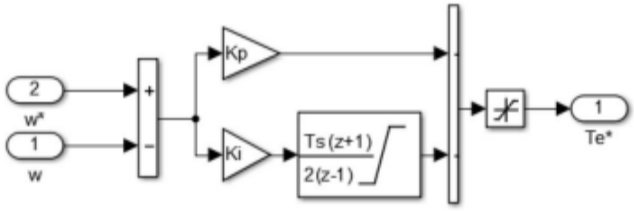

Fig. 3 Conventional PID controller block diagram

Here are the main contributions made as a result of this work: At the planned speeds and beyond, the main concern is to reduce the cost of the drive life cycle, and efficiency is an indicator of the cost of energy. The entire drive efficiency has an impact on the inverter's efficiency. The remainder of the paper is laid out as follows: The circuit is described in Section 2, and the control theory is explained in Section 3. Section 4 examines the power losses calculations and the efficiency of the IM drive. The modelling findings are reported in Section 5, the experimental data and the conclusion is made in Section 6.

II. CIRCUIT EXPLANATION

As depicted in Fig. 1, a battery EV is a self-contained electric vehicle that is made up of three basic components: for starters, an electric motor system, which often consists of a single electric machine, usually a three-part system.

The gear box and differential connect to the wheel. Second, there's a battery that acts as the power source; energy is chemically; the energy is chemically stored in the battery, which is connected to the gadget by an electrical DC/AC power adapter. Finally, the three-phase frequency and voltage control system, which is

connected via the accelerator and/or brake pedals, is applied to the electric machine, based on the present driver's request

The three-phase electric machine in Fig. 1 supplies traction power to the wheels. The left and right wheels will be torque by a differential with a gear ratio for high-speed adjustment of the electric motor shaft to the low speed of the wheels. An inverter controls the machine's speed by converting the battery voltage DC to three-phase AC electricity. When analyzing the energy consumption of an electric vehicle that is not part of the power chain from the mains to the wheels, it is crucial to take component losses into account. Our commitment is to provide adequate controllers for feedback in order to drive the EV system into the desired functionality. FLC approaches may be used to construct an insufficiently adaptive, flexible, and powerful controller for EV applications.

III. PRINCIPLE OF CONTROLLER

3.1 Conventional PID control

In the first design method, a traditional PID controller is provided for applying to an indirect field-oriented IM in order to regulate its speed and also the beginning scenario is explored The proposed control system incorporates (direct–quadrature–zero) conversion equations and a phase-locked loop algorithm that synchronizes with the utility current regulator, as shown in Fig. 2. The phase currents (i_a, i_b, i_c) are transformed to a d–q frame from a–b–c coordinates. The following conversions can be used to characterize the components of d–q.:

$$\begin{bmatrix} i_d \\ i_q \end{bmatrix} = \sqrt{\frac{2}{3}} \begin{vmatrix} \sin(wt) & \sin\left(wt - \frac{2\pi}{3}\right) & \sin\left(wt + \frac{2\pi}{3}\right) \\ \cos(wt) & \cos\left(wt - \frac{2\pi}{3}\right) & \cos\left(wt + \frac{2\pi}{3}\right) \end{vmatrix} \times \begin{bmatrix} i_{sa} \\ i_{sb} \\ i_{sc} \end{bmatrix} \quad (1)$$

Oscillation and average components are now included in the active and reactive power calculations. Two outer PID control loops, on the other hand, are used to obtain the average components of the active and reactive power outputs. Figure 3 shows a block schematic of a traditional PID controller. As seen in the conversions, this PID generates active current reference (i_d*) and reactive current reference (i_q*).:

$$i^*_d = k_p\left(P_{ref} - P\right) + k_i \int \left(P_{ref} - P\right) dt \quad (2)$$

$$i^*_q = k_p\left(Q_{ref} - Q\right) + k_i \int \left(Q_{ref} - Q\right) dt \quad (3)$$

Oscillation For the PID controllers used, k_p is the proportional constant and ki is the fundamental constant. P_{ref} is the charging power reference, while Q_{ref} is the reactive power required by the AC source as a reference value. The inner current loop and the outer voltage loop are integrated to provide the control. The current reference is created by comparing the current reference to the actual current in the outer loop, and it is used to regulate the inner loop. Therefore, the internal PID loops are created by comparing the measured line currents of the Park conversion. Operational relations in d - q coordinates are obtained by first summarizing the results (e_d and e_q) by the disengagement circumstances and then normalizing them by the DC voltage.

$$\begin{bmatrix} i_d \\ i_q \end{bmatrix} = \frac{1}{V_{dc}} \begin{vmatrix} e_d + v_d + 3wL \times i_q \\ e_q + v_q - 3wL \times i_d \end{vmatrix} \quad (4)$$

The duty ratios in (a–b–c) frame coordinates may be obtained via an inverse matrix transformation, which can be represented as follows. Exact continuous control rule.

$$\begin{bmatrix} D_a \\ D_b \\ D_c \end{bmatrix} = \sqrt{\frac{2}{3}} \begin{vmatrix} \sin(wt) & \cos(wt) \\ \sin\left(wt - \frac{2\pi}{3}\right) & \cos\left(wt - \frac{2\pi}{3}\right) \\ \sin\left(wt + \frac{2\pi}{3}\right) & \cos\left(wt + \frac{2\pi}{3}\right) \end{vmatrix} \times \begin{bmatrix} d_d \\ d_q \end{bmatrix} \quad (5)$$

3.2 Explanation of FLC

Controlling this problem remains a difficult challenge due to the nonlinear properties of AC motors, especially the squirrel cage induction motor (SCIM), because numerous parameters (most notably rotor resistances) fluctuate with operating circumstances. For EV applications, traditional control technology (PID) needs to be replaced by efficient intelligent FLC. Here are the most important factors to consider when designing a fuzzy system.

(i) Creation of fuzzy rules produced by professionals in the field for various control challenges
(ii) Select and adjust membership features;
(iii) Selecting the scaling factors.

The basic FLC was designed for EV applications in the second design approach, and it serves as a form of variable structure control unit that is well established for stability and endurance. A typical FLC is seen in Figure 4. Using the mathematical concept known as fuzzy logic, a novel way to improving adjustable speed drive voltage, frequency, and current regulation is offered. It may be used to solve difficulties in EV

applications where nonlinearity and its dynamic nature render traditional control approaches ineffective. This sort of difficulty has all of the features of motor control.

3.3 Speed control IM by using FLC

In the instance of motor speed control, FLC requires two input variables: the motor speed error (w_e) and its derivative, which reflects the speed variation error (w_e). The following is a description of speed error and speed variation error.

$$W_e = w_{ref}{}^* - w_{act} \qquad (6)$$

Where w^*_{ref} and w_{act} denote the reference motor speed and the actual/or measured motor speedrespectively

$$\frac{dwe}{dt} = \frac{\Delta we}{Ts} \qquad (7)$$

Where w^*_{ref} and w_{act} respectively indicate the reference speed of the motor and the actual speed measured of the motor::

$$\Delta u = \Delta t^* = k_1 \cdot we + k_2 \cdot \Delta we \qquad (8)$$

Where k1 and k2 denote the system's current and prior states, respectively. The universe of discourse is defined on the normalized domain [1, 1] in all membership functions of the controller inputs, i.e. we and we, and the output, i.e. u, as illustrated in Fig. 5. The fuzzy logic membership functions have been partitioned using five membership functions (MF) for the inputs and five MFs for the output fuzzy sets as shown in Fig.5.To relate two input variables to one output variable, a Mamdani fuzzy inference system is used in this system. The two input variables are the errors (we), which are the differences between the desired (set-point) and measured speed, and the change of error (Δ*we*). The scale factors Ge, Gde and Gu, in Fig.4, which perform the normalization process and demoralization of the specific variables of a conventional control gain.

When Ge, Gde, and Gu are the error measure, error variation, and FLC output factors, respectively, the value of these measurement factors is based on the initial error. As shown in Fig. 5, limited models are used to decrease the error and fluctuation in the error between (1, 1) the FLC input and output functions, while the FLC rules are recorded in Table 1. This feature suggests that instead of using NB, NS, Z, PS, and PB to represent negative big, negative small, zero, positive small, and positive large, you may use interpolation of the basic table of rules to produce a more Asymmetrical triangles with an equal base.

As illustrated in Table 1, each variable has five fuzzy subsets, resulting in 25 potential rules, the most common of which is: 'If e is NB and de is PB, then u is Z.' Because the perturbation technique changes the motor speed and output power, speed correction control is required. The motor output rotor speed should be kept as constant as possible.. As illustrated in Table 1, each variable has five fuzzy subsets, resulting in 25 potential rules, the most common of which is: 'If e is NB and de is PB, then u is Z.'

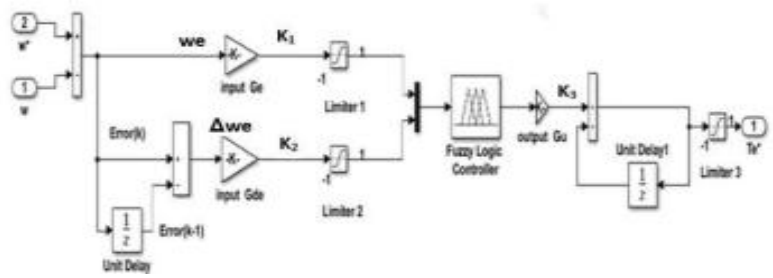

Figure 4: Construction of the fuzzy controller

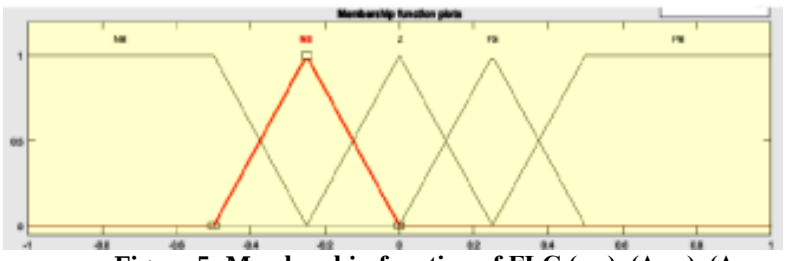

Figure 5: Membership function of FLC (we), (Δwe), (Δu

Table 1: Rules of the FLC

Δwe	we				
	NB	NS	Z	PS	PB
NB	NB	NB	NS	NS	Z
NS	NB	NS	NS	Z	PS

Z	NS	NS	Z	PS	PS
PS	NS	Z	PS	PS	PB
PB	Z	PS	PS	PB	PB

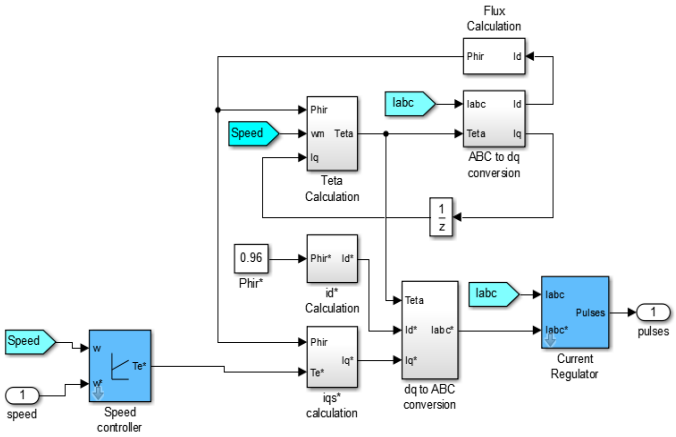

Figure 6: MATLAB model of three-phase IM

IV. POWER LOSS CALCULATIONS AND EFFICIENCY OF IM DRIVE

To validate the measured efficiency, the following power losses of the suggested control strategy at full load for a worst-case scenario are computed.

4.1 Parameters

Table 2 provides all of the supplied and derived parameters in this section. The parameters are taken from the data sheets usual values. Following that, some computed parameters will be displayed, with stray losses in being minimal.

4.2 Losses of input power

PID draws 62.6 A at 0.85 PF trailing for three-phase IM, whereas FLC draws 60 A at 0.85 PF lagging for FLC. The losses in input power can be calculated as follows:

$$P_{in} = 3\,V_L I_L \cos\theta$$
$$= 3\,V_{p\square} I_{p\square} \cos\theta \qquad (9)$$

4.3 Air-gap losses

The copper losses in the stator are 2 kW, and the core losses are 1.8 kW, both of which are taken into account. The power losses in the air gap may be calculated as follows:

$$P_{AG} = P_{IN} - (P_{SCl} + P_{Core}) = P_{Conv} + P_{RCL} \qquad (10)$$

Table 2: Given and calculated parameters

Item	Symbol	Value
voltage (line-to-line)	V_L	460 V
frequency	F	60 Hz
number of poles	P	4
power factor	PF	0.85 lagging
three-phase IM is drawing (PID)	I_L	62.6 A
three-phase IM is drawing (FLC)	I_L	60 A
stator copper losses (PID)	P_{SCL}	2 kW
stator copper losses (FLC)	P_{SCL}	1.8 kW
rotor copper losses (PID)	P_{RCL}	700 W
rotor copper losses (FLC)	P_{RCL}	500 W
core losses	P_{CORE}	1.8 kW
friction and windage losses	$P_{F\&W}$	600 W

Table 3: Comparision of PID and FLC

Item	Formulae	PID	FLC
Input Power	$P_{In} = \sqrt{3} \times V_L I_L \cos\theta$ $= 3 \times V_{P\square} I_{P\square} \cos\theta$	42.3947KW	40.6339KW
Air gap losses	$P_{AG} = P_{In} - (P_{SCL} + P_{Core})$	38.5947KW	37.0339KW
Converted power losses	$P_{Conv} = P_{AG} - P_{RCL}$	37.893KW	36.5339KW
Output Power	$P_{OUT} = P_{Conv} - (P_{F\&W}$ $- P_{Stray})$	37.295KW	35.934KW
Efficiency	$\eta = \frac{P_{OUT}}{P_{In}} \times 100$	87.97%	88.43%

4.4 Converted power losses

To calculated power converted, the only rotor copper losses are 700 W, is that taken into consideration. The converted power lossescan be estimated as

$$P_{CONV} = 3{I_2}^2 \frac{R_2\,(1-S)}{S} = (1-S)P_{AG} \qquad (11)$$

4.5 Output power losses

The calculation assumes no stray losses, thus the friction and windage losses are 600 W, which is what is taken into account. Table 3 shows how output power losses can be calculated.

$$P_{Out} = P_{Conv} - (P_{f\&w} + P_{Stray}) \qquad (12)$$

When the IM performs at its best, the energy efficiency rises. The proposed rules produce a worthy performance when compared to the results produced by the controller adjusted utilising certain known tuning rules.

V. SIMULINK RESULTS

Simulink and power sum toolboxes of MATLAB software are used in the simulation, where two cases have been considered as shown in Fig. 6. In the first case study, a 50 hp IM is powered using a PID controller. Three-phase voltage and current are measured and planned in the first 5 s of operation. Also, the probe is made in the acceleration curve and the resulting torque. In the second case, the motor itself is operated using FLC. PID controller response is compared with the FLC response and the results are shown inFigs. 7-9.

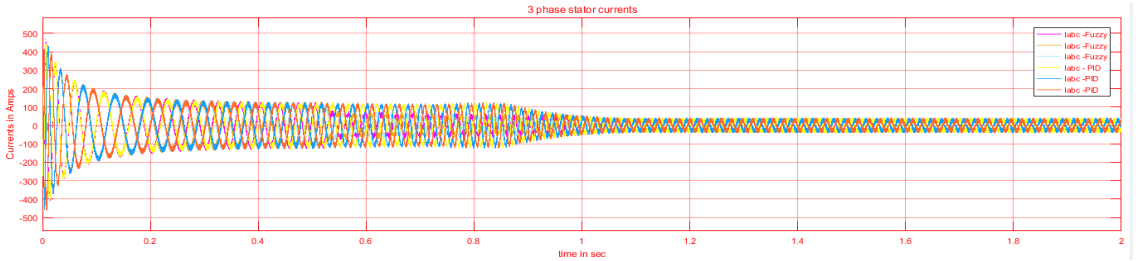

Figure 7: Three-phase stator current of PID and FLC models

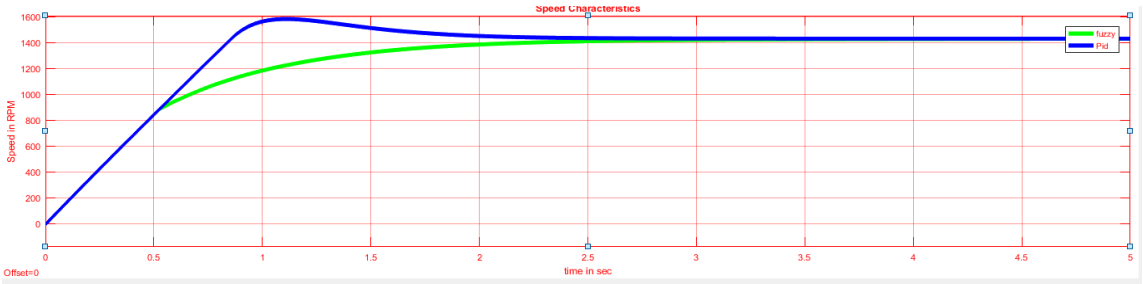

Figure 8: ***Simulation response of PID and FLC for rotor speed (rpm)***

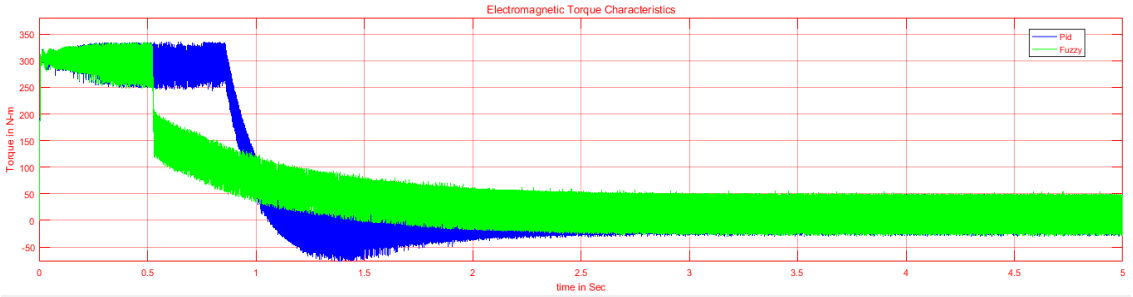

Figure 9: ***Simulation response of PID and FLC for electromagnetic torque (N m)***

When IM is not operating at maximum load, it might consume more power than is required. Heat is the result of this extra power. The initial current amplitude may be regulated using the FLC, allowing for better power savings during this period. The fuzzy controller's inputs are the speed error and change of error, which are employed in the outer loop to generate an equivalent controller term. A simulation analysis was done on a 50 hp IM-driven EV in this publication. Peak overshoot, steady-state error, rising time, and settling time are among the performance measures investigated. The findings revealed that the recommended system's phase current had fewer loss components (lower amplitude) but the same order components. In the steady state, the amplitudes of loss are lowered on average for the actual torque. It increases system performance by achieving a steady torque. In terms of rising time, settling time, and peak overshoot, the simulation results of the proposed FLC scheme revealed extremely strong stability and superior performance than the typical PID controller. The experimental results, which are in good agreement with the modelling results, support the suggested control system

References Speed ,rpm	Rise time, s		Settling time, s		Peak overshoot, %	
	FLC	PID	FLC	PID	FLC	PID
1432	0.731	0.681	1.982	2.584	0.501	10.55

VI. CONCLUSION

When IM operates in less than full load condition, it can consume more power than needed. This excess power is in the form of heat. By using the FLC the starting current amplitude can be controlled and more power can be saved during this time. The inputs of the fuzzy controller are the error of speed and change of error which are used in the outer loop for producing an equivalent controller term. In this paper, a simulation study was conducted on a 50 hp IM-driven EV. Different performance indicators are tested such as peak overshoot, steady-state error, rise time, and settling time. The results showed that the phase current in the suggested system includes fewer loss components (less amplitude) with the same order components. The amplitudes of loss are reduced on the average for the actual torque in the steady state. It achieves a smooth torque and improves system performance. The simulation results of the suggested FLC scheme showed very good stability and better performance over the conventional PID controller in rising time, settling time, and peak overshoot. The proposed control system is validated by the experimental results which are in good agreement with the simulation results.

REFERANCES

[1]. Buyukdegirmenci,V.T., Bazzi, A.M., Krein, P.T.: 'Evaluation of induction and permanent-magnet synchronous machines usingdrive-cycle energy and loss minimization in traction applications', IEEE Trans. Ind. Appl., 2014, 50, (1), pp. 395–403

[2]. Pal, A., Das, S.: 'A new sensorless speed estimation strategy for induction motor driven electric vehicle with energy optimization scheme'. IEEE 1st Int. Conf. on Power Electronics, Intelligent Control and Energy Systems (ICPEICES), Delhi, 2016, pp. 1–6

[3]. Lee, B.-S., Krishnan, R.: 'Adaptive stator resistance compensator for high performance direct torque controlled induction motordrives'. Conf. Record of 1998 IEEE Industry Applications Conf. Thirty-Third IAS Annual Meeting (Cat. No.98CH36242), St. Louis, MO, USA, 1998, vol. 1, pp. 423–430

[4]. Kunisetti, V.P.K., Meesala, R.E.K., Thippiripati, V.K.: 'Improvised predictive torque control strategy for an open end winding induction motor drive fed with four-level inversion using normalized weighted sum model', IET Power Electron., 2018, 11, (5), pp. 808–816

[5]. Hu, J., Dawson, D.M, Qu, Z.:'Adaptive tracking control of an induction motor with robustness to parametric uncertainty', IEE Proc., Electr. Power Appl., 1994, 141, (2), pp. 85–94

[6]. Kumar, R., Das, S., Chattopadhyay, A.K.: 'Comparative assessment of two different model reference adaptive system schemes for speed-sensorless control of induction motor drives', IET Electr. Power Appl., 2016, 10, (2), pp. 141–154

[7]. Sayed, K., Abo-Khalil, A.G., Alghamdi, A.S.: 'Optimum resilient operation and control dc microgrid based electric vehicles charging station powered by renewable energy sources', Energies, 2019, 12, (22), p. 4240